

A protection strategy for micro-grids based on positive-sequence component


ISSN 1752-1416

Received on 29th July 2014

Accepted on 6th January 2015

doi: 10.1049/iet-rpg.2014.0255

www.ietdl.org

Sohrab Mirsaedi, Dalila Mat Said , Mohammad Wazir Mustafa, Mohammad Hafiz Habibuddin

Centre of Electrical Energy Systems (CEES), Faculty of Electrical Engineering (FKE), Universiti Teknologi Malaysia (UTM), 81310 Skudai, Johor, Malaysia

✉ E-mail: dalilamatsaid@yahoo.com

Abstract: In recent years, the concept of micro-grid has appeared as an appropriate way for the integration of distributed energy resources (DERs) in the distribution networks. However, micro-grids have encountered a number of challenges from control and protection aspects. One of the main issues relevant to the protection of micro-grids is to develop a suitable protection technique which is effective in both grid-connected and stand-alone operation modes. This study presents a micro-grid protection scheme based on positive-sequence component using phasor measurement units and designed microprocessor-based relays (MBRs) along with a digital communication system. The proposed scheme has the ability to protect radial and looped micro-grids against different types of faults with the capability of single-phase tripping. Furthermore, since the MBRs are capable of updating their pickup values (upstream and downstream equivalent positive-sequence impedances of each line) after the first change in the micro-grid configuration (such as transferring from grid-connected to islanded mode and or disconnection of a line, bus or DER either in grid-connected mode or in islanded mode), they can protect micro-grid lines and buses against subsequent faults. Finally, in order to verify the effectiveness of the suggested scheme and the designed MBR, several simulations have been undertaken using DlgSILENT PowerFactory and MATLAB software packages.

1 Introduction

The recent progressions in technology and the increasing concerns associated with global warming have motivated researchers to explore cleaner and more efficient systems. To mitigate the negative influences of fossil fuel-based generation on the environment, a novel approach is to produce electricity by cleaner distributed energy resources (DERs) in the vicinity of the customers' sites [1–3]. For this reason, the utilisation of DERs such as wind turbines, photovoltaic systems, micro gas turbines and fuel cells has attracted more attention in recent years.

One suggested way for the integration of widespread proliferation of DERs is through micro-grids. Micro-grid is substantially defined as a collection of electrical/heat loads, parallel DERs and energy storage devices which can function in grid-connected or islanded mode [4–7]. The micro-grid protection philosophy is that it functions in grid-connected mode of operation under normal circumstances, but in case a fault takes place in the main grid side, it is disconnected from the rest of the network and is transferred to the islanded mode [8–10].

The most significant advantage of micro-grid is that it can provide high-reliability and high-quality power for the customers who need uninterrupted power supplies. In addition, a significant cost saving comes from the application of combined heat and power systems in micro-grids. Notwithstanding numerous advantages provided by micro-grids, they may pose some technical challenges which need to be fulfilled for researchers. Micro-grid protection and its entities is one of them [11–13]. Protection of micro-grids cannot be attained by the same philosophies which have traditionally been applied in distribution networks. The reason is that a protection scheme for micro-grids should take the followings into account: (a) bidirectional power flow in feeders; (b) existence of looped feeders; (c) decreased magnitude of the fault current in stand-alone operation mode [14–16]. As a result, the traditional overcurrent-based protection strategies are ineffective for micro-grids and some alternative strategies should be employed.

In a study by Oudalov and Fidigatti [17], an adaptive protection strategy was suggested, applying digital relaying and advanced communication technique. In the presented technique, the protection settings were updated periodically by means of micro-grid central controller in accordance with micro-grid operating modes. However, the proposed strategy necessitated updating or upgrading the protection devices which are presently applied in the distribution networks; moreover, fault calculations were relatively sophisticated for a micro-grid functioning in different modes. Dewadasa and his research group [18, 19] proposed an additional methodology for inverter-based micro-grids using an admittance relay with inverse time tripping characteristics. Despite the fact that the methodology had the ability to protect micro-grids either in grid-connected or in stand-alone mode, it was unable to protect micro-grids including rotating-based DERs. The further shortcoming of the strategy was that it was designed for only radial micro-grids. Tumilty *et al.* [20] and Redfern and Al-Nasseri [21] put forward a new protection approach based on voltage measurements to protect autonomous micro-grids against different kinds of faults. Nevertheless, the suggested approach did not take account of grid-connected operating mode as well as single-phase tripping. Jayawarna *et al.* [22, 23] proposed the installation of energy storage devices (such as batteries, flywheels etc.) within the micro-grid to equalise the magnitude of short-circuit current in both grid-connected and stand-alone modes of operation. By the application of such devices, micro-grid could still be protected using conventional overcurrent-based protection, but required adaptive protective devices. The major drawback of the proposed strategy was that the cost pertaining to such devices with high short-circuit capacity was extremely disadvantageous. In a study by Sortomme *et al.* [24], a differential based protection strategy was introduced which was able to protect micro-grids including radial or looped feeders in both modes of operations. However, the suggested strategy was only effective for the protection of lines and had not the ability to protect buses connected to DERs or loads. Nikkhajoei and Lasseter [25] established an alternative protection method based on

symmetrical components. The authors applied zero- and negative-sequence currents to protect micro-grids against asymmetrical faults. However, the suggested technique was ineffective in detecting three-phase faults; besides, the capability of single-phase tripping had not been taken into account in the method. Subsequently, in a research by Zamani *et al.* [26] another protection strategy was devised using zero- and negative-sequence components which had the ability to protect micro-grids against different kinds of faults; moreover, the proposed strategy did not require communication system. The main problem associated with the proposed method was that it was dependent on the micro-grid configuration, because the method had been designed for only radial micro-grids and was not capable of protecting micro-grids containing looped feeders; furthermore, because of the need for zero-sequence current in the proposed method, its implementation necessitated the application of a specific type of transformer (only grounded transformers) inside the micro-grid.

This paper presents a micro-grid protection scheme based on positive-sequence component using phasor measurement units (PMUs) and designed microprocessor-based relays (MBRs) along with a digital communication system. The proposed scheme has the ability to protect radial and looped micro-grids against different types of faults with the capability of single-phase tripping. Furthermore, since the MBRs are capable of updating their pickup values after the first change in the micro-grid configuration, they can protect micro-grid lines and buses against subsequent faults.

The remainder of this paper is organised as follows: in Section 2, technical challenges in the protection of micro-grids are discussed; Section 3 describes the proposed protection scheme; in Section 4, different parts of the designed MBR are introduced; Section 5 is dedicated to the simulation results; and finally, Section 6 concludes this paper.

2 Technical challenges in the protection of micro-grids

The majority of the distribution networks are designed to operate in radial mode, in which the power flows in one direction from higher-voltage levels to lower-voltage levels. Owing to this, the protection of such networks is accomplished using simple and relatively low-cost overcurrent-based protective devices such as overcurrent relays, reclosers and fuses. When a micro-grid is formed in a distribution network, the configuration is changed to a complicated multi-source power system. The protection of micro-grid should be in such a way that a safe and secure protection is provided in both grid-connected and stand-alone operation modes [27, 28]. Nevertheless, the function of micro-grid in these two modes creates some new protection problems. During grid-connected operation mode, since micro-grid provides a large short-circuit current to the fault point, the protection can be performed by existing protective devices within the distribution networks, but in islanded mode, fault currents are drastically lower than those of grid-connected mode. The reason is that the Thevenin's impedance viewed from the fault point in islanded operating mode is much higher than that of grid-connected mode; hence, the employment of traditional overcurrent-based protective devices in micro-grids is no longer valid and some alternative protection schemes should be developed.

Table 1 Existence of symmetrical components during different types of faults

Fault type	Positive-sequence	Negative-sequence	Zero-sequence
single line to ground	yes	yes	yes
line to line	yes	yes	no
line to line to ground	yes	yes	yes
three phase	yes	no	no

3 Proposed protection scheme

This paper presents a protection scheme for micro-grids using PMUs and designed MBRs, thereby detecting different kinds of faults in both grid-connected and islanded modes of operation. In the proposed protection scheme, PMUs which are responsible for extracting voltage and current phasors (magnitudes and their respective phasor angles) based on digital sampling of alternating current (AC) waveforms are installed at both ends of each line of micro-grid. Subsequently, the information extracted by PMUs of each line is transferred to the MBR of that line through a digital communication system. After a fault incident within the micro-grid, the information received by PMUs in all MBRs is analysed, and then the fault occurrence, location of fault and faulted phases are recognised by the relevant MBR or MBRs. Subsequently, depending on the fault type, proper tripping signals are issued to the relevant circuit breakers.

3.1 Detection of fault incident

To detect different types of faults, this paper presents a protection scheme based on symmetrical components approach. The approach, developed by Fortescue, is one of the most effective ones which is applied to transform a three-phase unbalanced system into three sets of symmetrically balanced phasors, namely positive-, negative- and zero-sequence components. In case a fault strikes within a network, these symmetrical components are formed depending on the fault type. Table 1 illustrates the existence of symmetrical components during different types of faults. As can be seen from this table, the positive-sequence is the only component which exists in all types of faults. For this reason, in this paper, the positive-sequence component is employed to detect different kinds of faults.

3.2 Detection of fault location

As mentioned earlier, the majority of the proposed methods to date are strongly dependent on the micro-grid configuration. To possess an appropriate method having the ability to protect different micro-grids with different configurations, micro-grid feeders should be sectionalised in such a way that each section (micro-grid's line or bus) is protected independent of other sections. To fulfil this, the upstream and downstream of each line are replaced with its upstream and downstream equivalent circuits, respectively. Both of these equivalent circuits include a voltage source in series with impedance. Fig. 1 indicates the upstream and downstream equivalent circuits of Line 12 of a typical micro-grid during a fault.

During a fault occurrence in Line 12 of Fig. 1, different symmetrical components are created depending on the fault type. The equivalent circuit diagram in the system of symmetrical components for different kinds of faults by considering upstream and downstream equivalent circuits are depicted in Fig. 2.

By replacing the equivalent impedance of negative- and zero-sequence networks between terminals AB of positive-sequence network for all types of faults, a general model for the analysis of different kinds of faults can be developed. The developed model is demonstrated in Fig. 3, in which impedance $Z_{eq2,0}$ is the representative of negative- and zero-sequence networks.

Depending on the fault type, the value of the impedance is different. Equation (1) expresses the value of impedance $Z_{eq2,0}$ for different types of faults

$$Z_{eq2,0} = \begin{cases} Z_{eq0} + Z_{eq2}, & \text{for single line to ground faults} \\ Z_{eq2}, & \text{for line to line faults} \\ Z_{eq0} || Z_{eq2}, & \text{for line to line to ground faults} \\ 0, & \text{for three-phase faults} \end{cases} \quad (1)$$

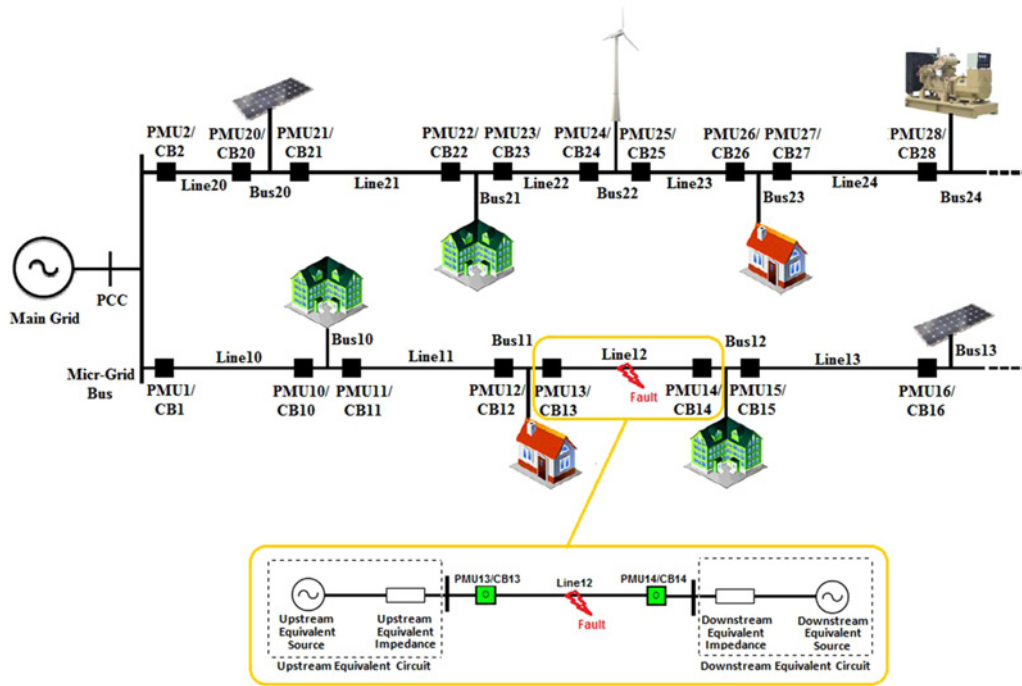


Fig. 1 Upstream and downstream equivalent circuits of Line12 of a typical micro-grid during a fault

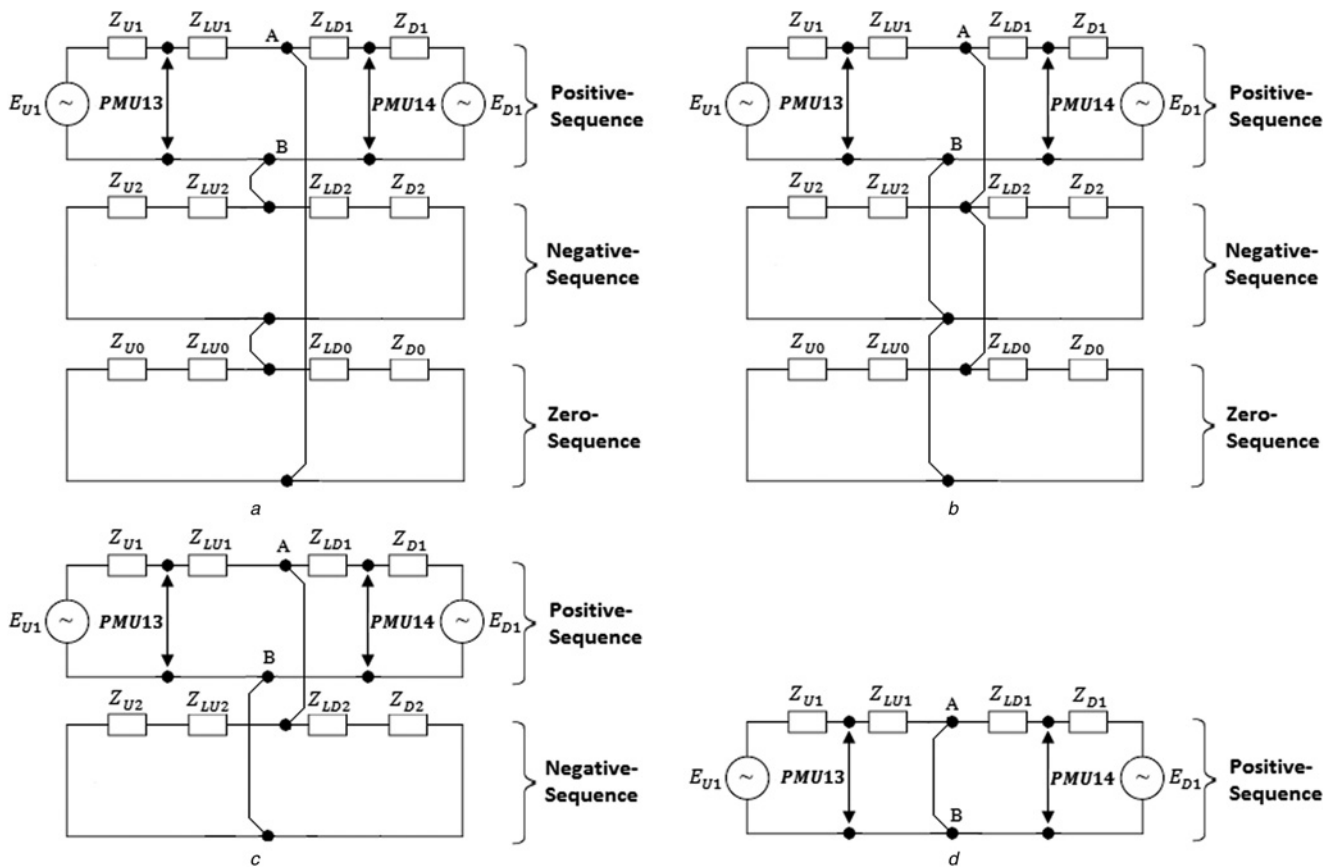


Fig. 2 Equivalent circuit diagram in the system of symmetrical components by considering upstream and downstream equivalent circuits for

- a Single line to ground fault
- b Line to line to ground fault
- c Line to line fault
- d Three-phase fault

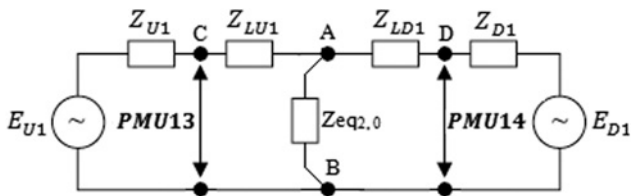


Fig. 3 Developed general model for the analysis of different kinds of faults

where

$$Z_{eq0} = (Z_{U0} + Z_{LU0}) || (Z_{D0} + Z_{LD0})$$

$$Z_{eq2} = (Z_{U2} + Z_{LU2}) || (Z_{D2} + Z_{LD2})$$

In the proposed protection scheme, after the detection of fault incident, the faulted section is recognised by the developed model of Fig. 3 in such a way as to compare the value of upstream and downstream equivalent positive-sequence impedances, before and after the fault. In fact, when a fault occurs inside a line, impedance $Z_{eq2,0}$ is created between points C and D. Therefore the values of both upstream and downstream equivalent positive-sequence impedances after the fault (Z_{U1} , Z_{D1}) remain equal to the values of those impedances before the fault ($Z_{U1(pre)}$, $Z_{D1(pre)}$), but in case a fault occurs at the upstream or downstream of a line, respectively, only the value of Z_{D1} or only the value of Z_{U1} remains constant after the fault.

It should be noted that, in the proposed protection scheme, since the total positive-sequence impedance of each line is calculated using the positive-sequence voltage and current phasors, obtaining time-synchronised measurements from its both ends is necessary. However, in short distribution lines, the proposed scheme can function without the need for PMUs.

Fig. 4 demonstrates the single-phase diagram of the proposed protection scheme for Line 12 of the micro-grid shown in Fig. 1. According to this figure, after a fault occurrence inside of Line12, both values of Z_{U1} and Z_{D1} of MBR_Line12 remain constant; in fact, both PMU13 and PMU14 see the fault in their forward side, so PMU13 and PMU14 Forward Fault Trip signals from MBR_Line12 are issued to both CB13 and CB14, but in case of a fault at Bus11, the values of Z_{D1} of MBR_Line12 and Z_{U1} of MBR_Line11 remain constant, so PMU12 and PMU13 Reverse Fault Trip signals are issued, respectively, from MBR_Line11 and MBR_Line12, and disconnect CB12 and CB13. Similarly, in case of a fault incident at Bus12, PMU14 and PMU15 Reverse Fault Trip signals are issued, respectively, from MBR_Line12 and MBR_Line13 and disconnect CB14 and CB15.

As can be seen in this figure, the back-up protection is also provided in such a way that after any failure in the main protection of each line or bus, the disconnection signals are issued to its adjacent circuit breakers after a pre-determined time delay to isolate the smallest possible faulted area.

4 Designed MBR

Fig. 5 displays the schematic diagram of MBR_Line12. As can be seen in this figure, it consists of four main parts, namely, fault incident detector, fault locator, faulty phase detector and blocking signal issue-maker, each of which are described in detail in the following sections.

4.1 Fault incident detector

As explained earlier, the positive-sequence component is the only component which exists in all types of faults. Therefore, in the proposed protection scheme, the component is used to detect

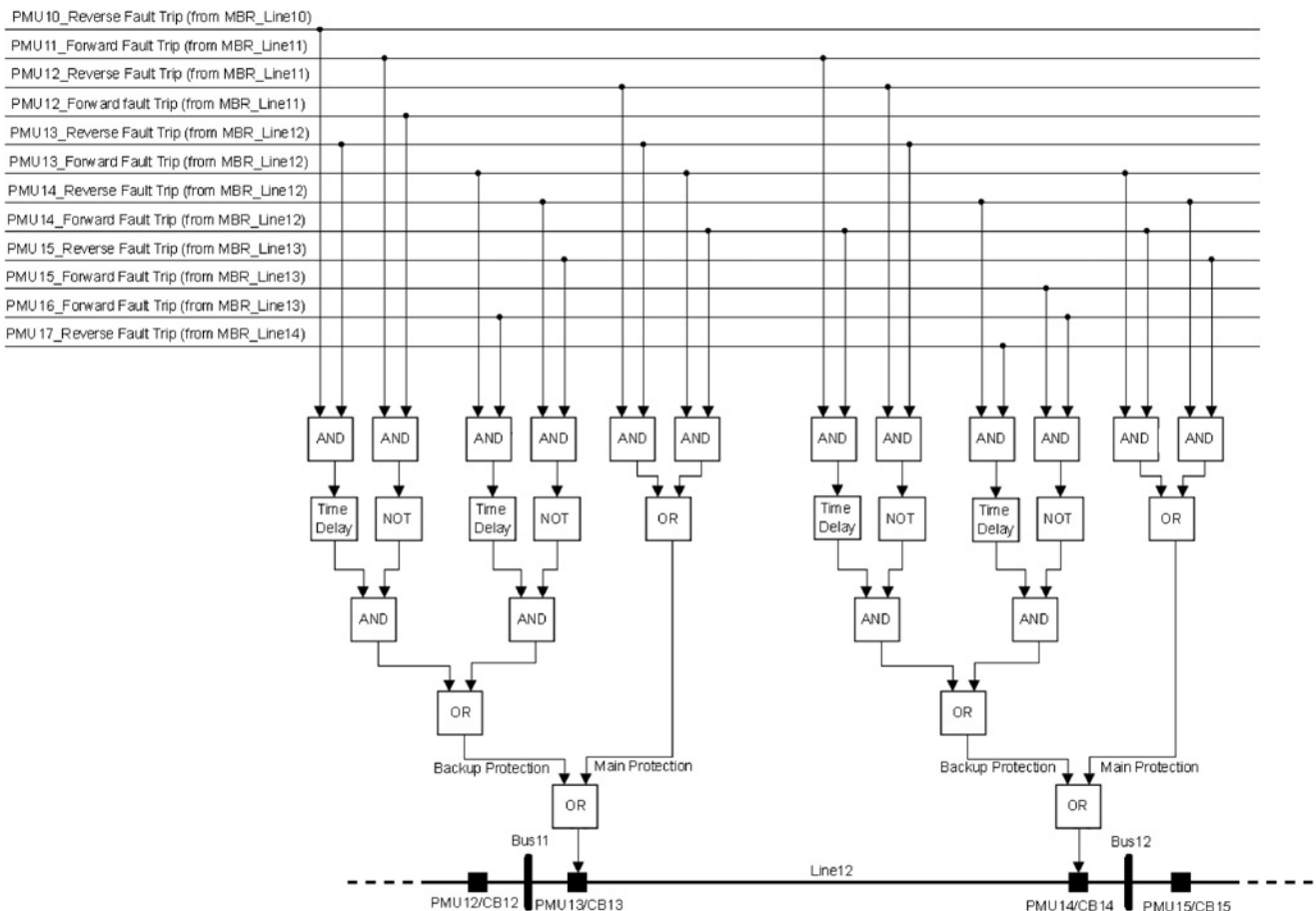


Fig. 4 Single-phase diagram of the proposed protection scheme for Line 12 of the micro-grid shown in Fig. 1

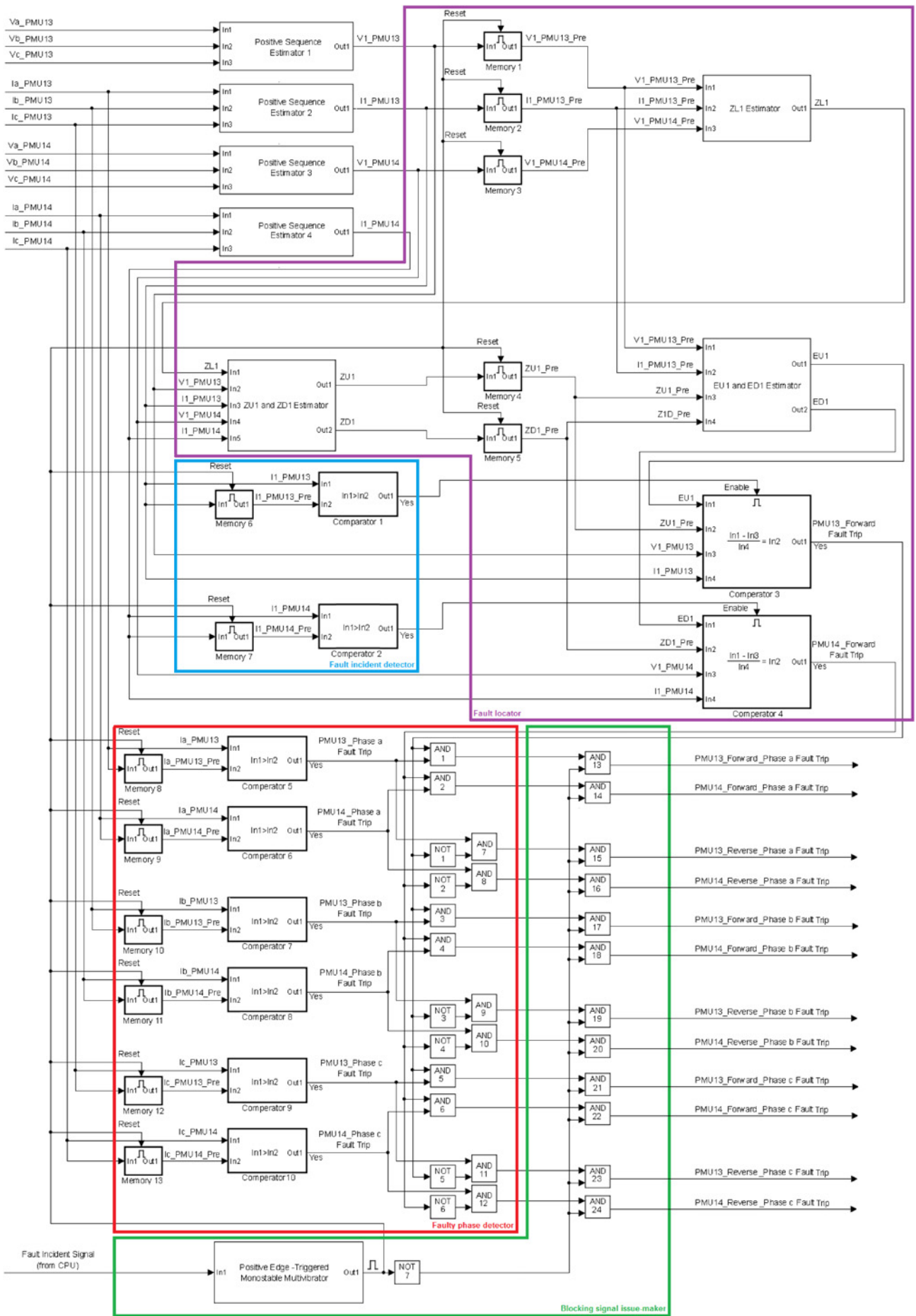


Fig. 5 Schematic diagram of MBR_Line12

different kinds of faults. When a fault occurs in a micro-grid section (line or bus), the positive-sequence current magnitude of that section is increased; hence, the fault occurrence can be detected by comparing the magnitude before and after the fault.

In the designed MBR, for the detection of fault in each line and its adjacent buses, a fault incident detector is allocated. However, since a fault in one section may increase the positive-sequence current magnitude of other sections, MBRs related to non-faulted lines may issue fault trip signals mistakenly. Hence, the deployment of an additional detector (fault locator) is necessary.

4.2 Fault locator

As mentioned in Section 3.2, the faulted section is identified based on changes in the values of upstream and downstream equivalent positive-sequence impedances before and after the fault. In the designed MBR, this function is performed by fault locator. Prior to fault incident, the fault locator respective to MBR of each line, first, calculates the values of Thevenin's equivalent positive-sequence impedances (TEPSIs) at both ends of that line, and then it deploys the values to determine the values of impedances $Z_{U1(pre)}$ and $Z_{D1(pre)}$.

Finally, the faulted section can be recognised by comparing the values of upstream and downstream equivalent positive-sequence impedances before ($Z_{U1(pre)}$, $Z_{D1(pre)}$) and after (Z_{U1} , Z_{D1}) the fault.

To determine the TEPSI of each point within the micro-grid, this paper introduces an online methodology using three consecutive voltage and current measurements of PMUs at different time instants. Since any changes in the frequency of the micro-grid system will lead to slip between micro-grid frequency system and the PMU sampling frequency, phase angles of voltage and current for these three measurements will be different.

On the basis of Thevenin's model, the node positive-sequence voltage equation is defined as

$$V_1 = E_{t1} - Z_{t1} \cdot I_1 \tag{2}$$

According to (2), the positive-sequence voltage equation for PMU13 terminals becomes

$$V_{1PMU13} = E_{t1PMU13} - Z_{t1PMU13} \cdot I_{1PMU13} \tag{3}$$

where $E_{t1PMU13}$ = Thevenin's equivalent positive-sequence voltage source at PMU13 terminals, $Z_{t1PMU13}$ = TEPSI at PMU13 terminals.

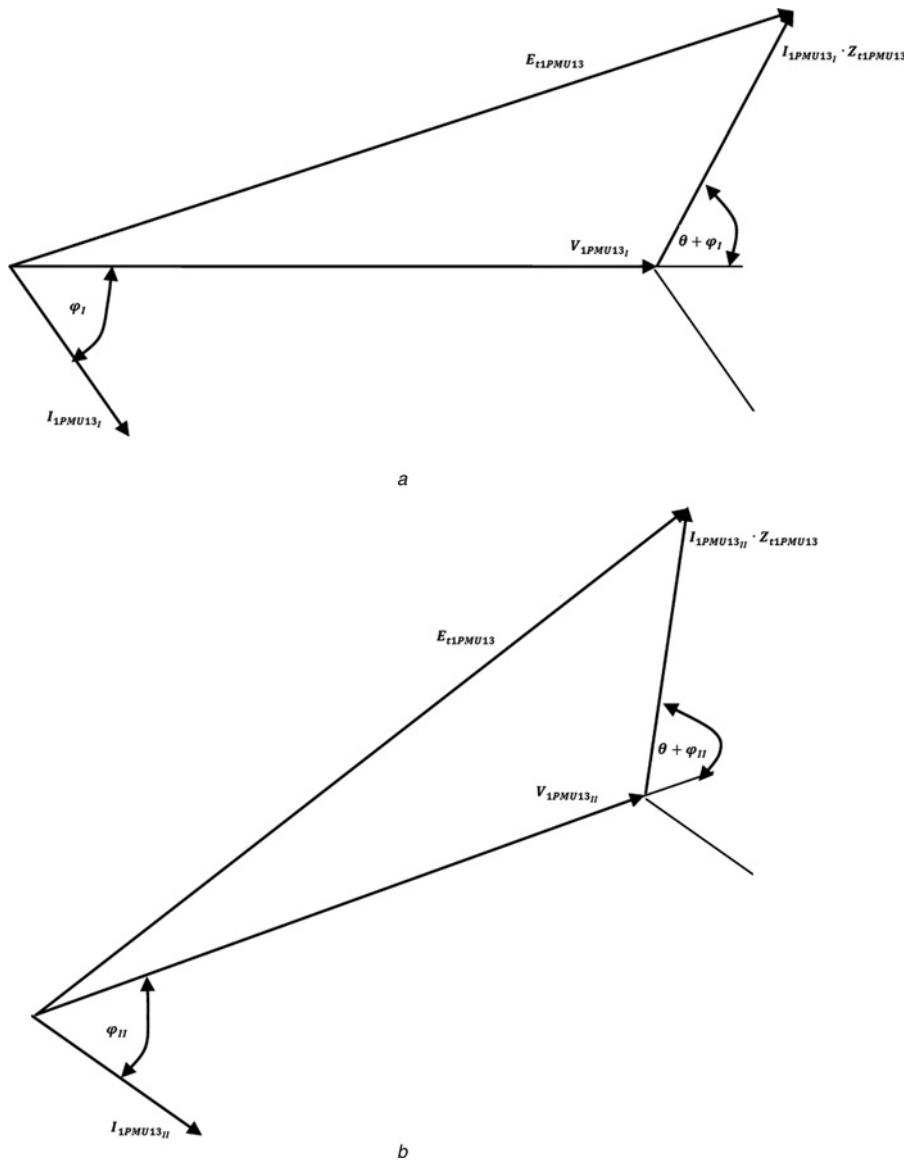


Fig. 6 Positive-sequence phasor diagrams for two different measurements at PMU13 terminals

a 1st measurement
b IInd measurement

Positive-sequence phasor diagrams of (3) for two different measurements at PMU13 terminals are indicated in Fig. 6.

Since $E_{t1PMU13}$ is the Thevenin's positive-sequence equivalent voltage source, its magnitude for both measurements are identical, but its angle in the IInd measurement is shifted by an angle equal to the phase drift. Referring to Fig. 6, $E_{t1PMU13}$ equation for the Ist measurement can be written as

$$E_{t1PMU13}^2 = V_{1PMU13_I}^2 + I_{1PMU13_I}^2 \cdot Z_{t1PMU13}^2 + 2V_{1PMU13_I} \cdot I_{1PMU13_I} \cdot Z_{t1PMU13} \cdot \cos(\theta + \varphi_1) \quad (4)$$

By expanding $\cos(\theta + \varphi_1)$, (4) can be expressed as follows

$$E_{t1PMU13}^2 = V_{1PMU13_I}^2 + I_{1PMU13_I}^2 \cdot Z_{t1PMU13}^2 + 2P_{1PMU13_I} \cdot R_{t1PMU13} - 2Q_{1PMU13_I} \cdot X_{t1PMU13} \quad (5)$$

where $R_{t1PMU13}$ and $X_{t1PMU13}$ denote the resistance and reactance of the TEPSI, as well as P_{1PMU13_I} and Q_{1PMU13_I} , which, respectively, represent active and reactive powers flowing through Line 12. Similarly, the $E_{t1PMU13}$ equation for the IInd measurement can be written as

$$E_{t1PMU13}^2 = V_{1PMU13_{II}}^2 + I_{1PMU13_{II}}^2 \cdot Z_{t1PMU13}^2 + 2P_{1PMU13_{II}} \cdot R_{t1PMU13} - 2Q_{1PMU13_{II}} \cdot X_{t1PMU13} \quad (6)$$

By subtracting (6) from (5)

$$V_{1PMU13_I}^2 - V_{1PMU13_{II}}^2 + (I_{1PMU13_I}^2 - I_{1PMU13_{II}}^2) \cdot Z_{t1PMU13}^2 + 2(P_{1PMU13_I} - P_{1PMU13_{II}}) \cdot R_{t1PMU13} - 2(Q_{1PMU13_I} - Q_{1PMU13_{II}}) \cdot X_{t1PMU13} = 0 \quad (7)$$

Equation (7) can be arranged as follows

$$\begin{aligned} & \left(R_{t1PMU13} + \frac{P_{1PMU13_I} - P_{1PMU13_{II}}}{I_{1PMU13_I}^2 - I_{1PMU13_{II}}^2} \right)^2 \\ & + \left(X_{t1PMU13} - \frac{Q_{1PMU13_I} - Q_{1PMU13_{II}}}{I_{1PMU13_I}^2 - I_{1PMU13_{II}}^2} \right)^2 \\ & = \frac{V_{1PMU13_{II}}^2 - V_{1PMU13_I}^2}{I_{1PMU13_I}^2 - I_{1PMU13_{II}}^2} + \frac{(P_{1PMU13_I} - P_{1PMU13_{II}})^2}{(I_{1PMU13_I}^2 - I_{1PMU13_{II}}^2)^2} \\ & + \left(\frac{Q_{1PMU13_I} - Q_{1PMU13_{II}}}{I_{1PMU13_I}^2 - I_{1PMU13_{II}}^2} \right)^2 \end{aligned} \quad (8)$$

This is the equation of a circle in the positive-sequence impedance plane which indicates a locus for the TEPSI seen from PMU13 terminals. As it does not specify a certain value for $Z_{t1PMU13}$, a third measurement is required so that it is used with the first and second measurements to create another two circles for $Z_{t1PMU13}$. Fig. 7 shows the positive-sequence impedance plane including the circles obtained from three different measurements. As shown in Fig. 7, the value of TEPSI seen from PMU13 terminals is specified by the intersection of the three circles.

According to Thevenin's theorem, Thevenin's equivalent impedance for any two-terminal of the network is the impedance seen from those terminals when the sources are set to zero. Hence, $Z_{t1PMU13}$ for PMU13 terminals prior to fault incident is equivalent to $Z_{U1} \parallel (Z_{L1} + Z_{D1})$. By setting this equal to the calculated $Z_{t1PMU13}$ from the intersection point of the three circles

$$Z_{t1PMU13_{cal.}} = Z_{U1} \parallel (Z_{L1} + Z_{D1}) \quad (9)$$

By following the same procedure for PMU14 terminals prior to fault incident

$$Z_{t1PMU14_{cal.}} = Z_{D1} \parallel (Z_{L1} + Z_{U1}) \quad (10)$$

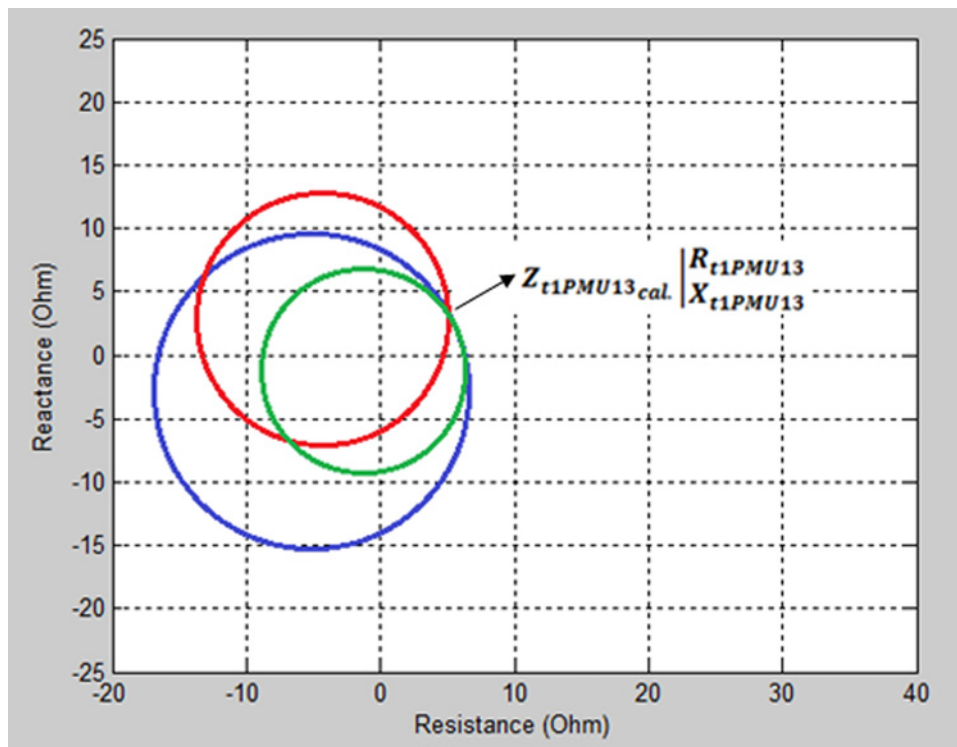


Fig. 7 Positive-sequence impedance plane including the circles obtained from three different measurements

By solving (9) and (10), the values of $Z_{U1(pre)}$ and $Z_{D1(pre)}$ are obtained. Subsequently, the fault locator respective to each line compares the values of $Z_{U1(pre)}$ and $Z_{D1(pre)}$ with the values of Z_{U1} and Z_{D1} after the fault incident and identifies the faulted section.

4.3 Faulty phase detector

Single-phase tripping capability has long been regarded as an effective way of improving system security and reliability. It leads to removal of unnecessary interruptions of the unaffected phases in case the fault does not involve all three phases. In the designed MBR, having detected the faulted section by means of the fault locator, the affected phases of that section are identified through faulty phase detector. The faulty phase detector compares the current magnitude of each phase of the faulted section before and after the fault, and then issues the proper disconnection signals to the relevant circuit breakers of that section.

4.4 Blocking signal issue-maker

To update the values of $Z_{U1(pre)}$ and $Z_{D1(pre)}$ as well as precluding from mal-operation of MBRs for the subsequent faults, a blocking

signal issue-maker has been considered. In fact, after the isolation of the first fault (inside or outside of micro-grid) a fault incident signal is issued from the disconnected circuit breakers to the central protection unit (CPU). Afterwards, CPU sends the signal to all MBRs in the micro-grid. The signal is responsible for resetting the memories as well as blocking the outputs of all MBRs until the new values of $Z_{U1(pre)}$ and $Z_{D1(pre)}$ are determined. To fulfil this, a positive edge-triggered monostable multivibrator is used. Once it received a fault incident signal resulted from the disconnection of circuit breakers, generates an output pulse with the duration of T . It is clear that the duration of the pulse should be more than the time which is needed so that the values of $Z_{U1(pre)}$ and $Z_{D1(pre)}$ are updated.

5 Simulation results

To evaluate the effectiveness of the proposed scheme and the designed MBR, several simulations have been carried out using DigSILENT PowerFactory and MATLAB software packages. The configuration of the simulated micro-grid, which hereinafter is

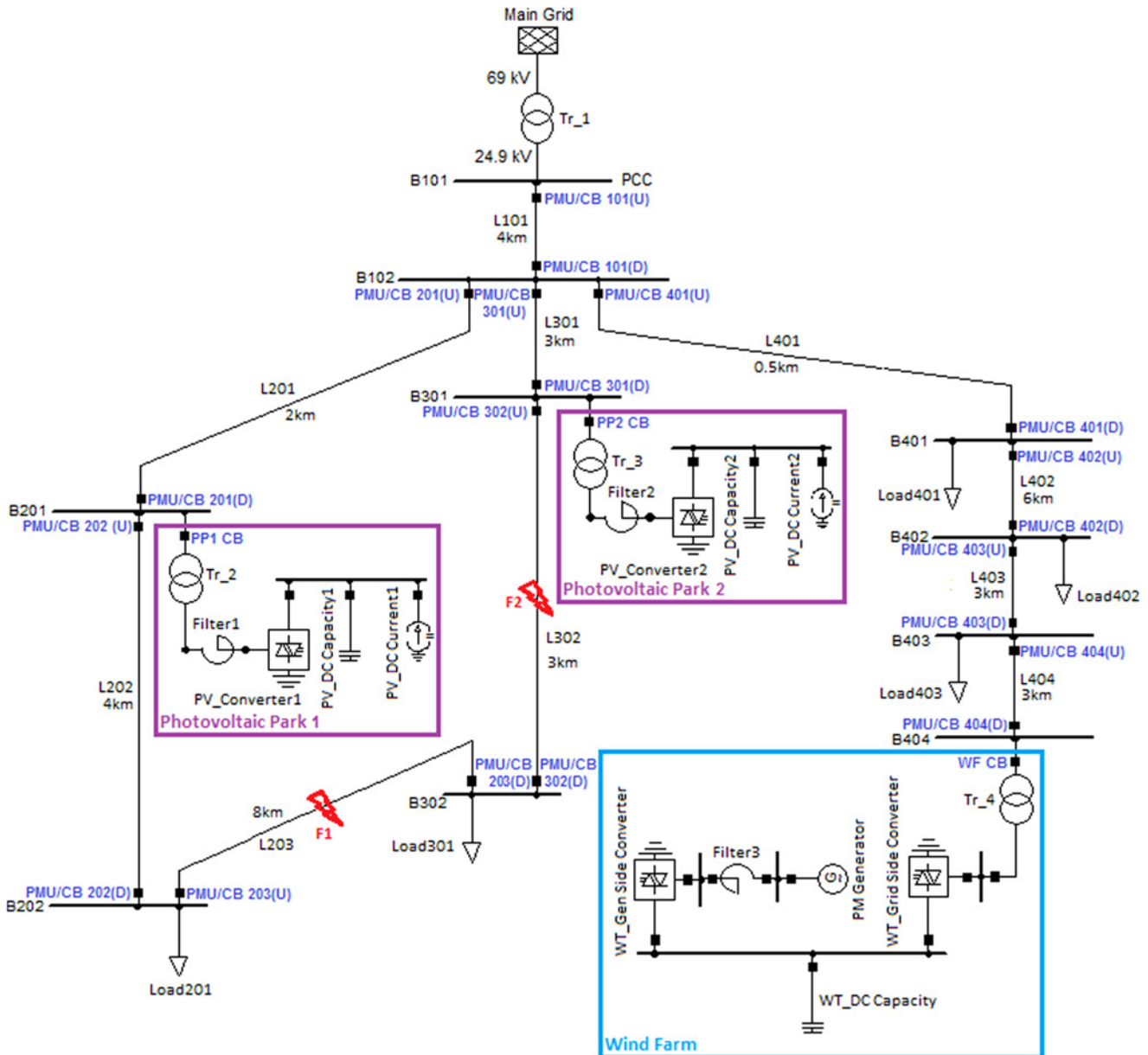


Fig. 8 Single-line diagram of the study micro-grid

referred to as ‘study micro-grid’ as well as the case studies are presented in the following sections.

5.1 Study micro-grid

The single-line diagram of the study micro-grid is illustrated in Fig. 8. As can be seen in this figure, the study micro-grid is connected to the main grid by means of a 69 kV/24.9 kV Dyn transformer. It also includes two photovoltaic parks (640 kW) and one wind farm (504 kW) which are interfaced with the network through respective YNyn transformers. The information associated with the applied transformers and loads of the study micro-grid is listed in Tables 2 and 3.

5.2 Case studies

To prove the efficacy of the proposed protection scheme in the grid-connected and islanded operating modes, the performance of several MBRs was simulated, but because of space restriction and format requirements of this publication, only the simulation results of MBR_Line203 is included in this paper. The simulation results showed that the suggested protection scheme can provide a robust protection against different kinds of faults.

Table 2 Information associated with the applied transformers in the study micro-grid

Transformer type	HV ^a , kV	LV ^b , kV	Vector group
Tr-1	69	24.9	Dyn0
Tr-2	24.9	0.4	YNyn0
Tr-3	24.9	0.4	YNyn0
Tr-4	24.9	0.4	YNyn0

^aHigh voltage, ^bLow voltage

Table 3 Information associated with the loads in the study micro-grid

Name	Phase A		Phase B		Phase C	
	kW	kVAR	kW	kVAR	kW	kVAR
Load201	100	16	75	14	30	3
Load301	175	22	53	18	10	2
Load401	14	5	77	13	21	7
Load402	93	26	24	10	18	5
Load403	111	38	28	3	12	6

Table 4 Simulation results of MBR_Line203 during different kinds of faults at the midpoints of Lines 203 and 302 (F1 and F2 in Fig. 8) in the grid-connected operating mode

Fault type	AG ^a		BC ^b		BCG ^c		ABC ^d		
	F1	F2	F1	F2	F1	F2	F1	F2	
PMU203 (U)	$ V_{1PMU203(U)} $, kV	11.5966	11.935	9.6348	10.3793	8.4334	9.3542	5.5298	7.0634
	$ E_{U1} - V_{1PMU203(U)} $, kV	2.7971	2.4659	4.7554	4.0319	5.9731	5.0408	8.8869	7.3347
	$ I_{1PMU203(U)} $, A	319.6722	281.8203	543.4804	460.7938	682.6478	576.098	1015.657	838.261
	$ I_{APMU203(U)} $, A	930.9764	782.8649	3.1912	3.18577	3.11	3.1634	1023.2251	840.832
	$ I_{BPMU203(U)} $, A	3.2012	3.2266	940.2354	794.6089	1001.0088	821.6507	1032.0562	847.7558
PMU203 (D)	$ V_{1PMU203(D)} $, kV	11.6082	10.7275	9.6623	8.094	8.4671	6.4597	5.5934	2.4528
	$ E_{D1} - V_{1PMU203(D)} $, kV	2.7872	3.6819	4.7308	6.3265	5.9364	8.0298	8.8155	11.9826
	$ I_{1PMU203(D)} $, A	325.9221	489.6217	553.3164	863.8151	694.3239	1118.3574	1031.0646	1756.9881
	$ I_{APMU203(D)} $, A	930.5706	1410.607	3.1866	3.1499	3.176	3.0042	1032.2881	1750.8619
	$ I_{BPMU203(D)} $, A	3.3172	3.3023	959.952	1488.0535	1021.8158	1630.9718	1033.3917	1758.9912
	$ I_{CPMU203(D)} $, A	3.3204	3.3186	961.2623	1484.2312	1021.4874	1687.068	1028.5264	1753.9268
$Z_{U1L203} = \frac{ E_{U1} - V_{1PMU203(U)} }{ I_{1PMU203(U)} }$, Ω		≈8.7499	≈8.7499	≈8.7499	≈8.7499	≈8.7499	≈8.7499	≈8.7499	≈8.7499
$Z_{D1L203} = \frac{ E_{D1} - V_{1PMU203(D)} }{ I_{1PMU203(D)} }$, Ω		≈8.5499	≈8.5499	≈8.5499	≈8.5499	≈8.5499	≈8.5499	≈8.5499	≈8.5499
operated CBs in Line 203	phase A	yes	no	no	no	no	no	yes	no
	phase B	no	no	yes	no	yes	no	yes	no
	phase C	no	no	yes	no	yes	no	yes	no

^aLine A to ground fault, ^bLine B to line C fault, ^cLine B to line C to ground fault, ^dThree-phase fault

According to the simulation results, the calculated values of upstream and downstream equivalent positive-sequence impedances (from the intersection of circles) for Line 203 before the fault incidents in both grid-connected and islanded operating modes are as follows

$$Z_{U1L203 (pre).cal.} = \begin{cases} 8.7499 \Omega, & \text{for grid-connected mode} \\ 47.1347 \Omega, & \text{for islanded mode} \end{cases}$$

$$Z_{D1L203 (pre).cal.} = \begin{cases} 8.5499 \Omega, & \text{for grid-connected mode} \\ 77.059 \Omega, & \text{for islanded mode} \end{cases}$$

where $Z_{U1L203 (pre).cal.}$ = upstream equivalent positive-sequence impedance of PMU203 (U), $Z_{D1L203 (pre).cal.}$ = downstream equivalent positive-sequence impedance of PMU203 (D).

Tables 4 and 5 indicate the simulation results of MBR_Line203 during different kinds of faults at the midpoint of Lines 203 and 302 (F1 and F2 in Fig. 8) in both grid-connected and islanded operating modes, respectively.

As can be seen from these tables, the positive-sequence current magnitudes during different types of faults in islanded mode are drastically lower than those of grid-connected mode. It is due to the fact that the Thevenin’s impedance viewed from the fault points (F1 and F2) in islanded operating mode is much higher than that of grid-connected mode; therefore, traditional over-current strategies with a single setting group will not be able to provide selective trips for all types of faults in both grid-connected and islanded modes of operation.

Once fault F1 or F2 occurred either in grid-connected or islanded mode, MBR_Line203 calculates the values of Z_{U1L203} and Z_{D1L203} and then compares them, respectively, with the values of $Z_{U1L203 (pre).cal.}$ and $Z_{D1L203 (pre).cal.}$. According to Tables 4 and 5, since Fault F1 has occurred inside of Line 203, the values of Z_{U1L203} and Z_{D1L203} are, respectively, equal to the values of $Z_{U1L203 (pre).cal.}$ and $Z_{D1L203 (pre).cal.}$, whereas fault F2 has occurred at the downstream of Line 203, and therefore only the value of Z_{U1L203} is equal to the value of $Z_{U1L203 (pre).cal.}$

6 Conclusion

This paper proposed a protection strategy based on positive-sequence component for micro-grids. The proposed strategy which addresses the protection issues of a micro-grid in both modes of operation is implemented through PMUs and

Table 5 Simulation results of MBR_Line203 during different kinds of faults at the midpoints of Lines 203 and 302 (F1 and F2 in Fig. 8) in the islanded operating mode

Fault type		AG		BC		BCG		ABC	
		F1	F2	F1	F2	F1	F2	F1	F2
PMU203 (U)	$ V_{1PMU203(U)} $, kV	11.0988	11.3099	9.1148	9.743	7.7168	8.4308	4.73	5.9963
	$ E_{U1} - V_{1PMU203(U)} $, kV	3.2179	2.9887	5.164	4.5415	6.5494	5.8419	9.5093	8.2544
	$ I_{1PMU203(U)} $, A	68.2702	63.4076	109.5583	96.3515	138.9507	123.9405	201.7473	175.1235
	$ I_{APMU203(U)} $, A	175.7082	159.1533	3.3477	3.3381	3.2157	3.275	201.6867	175.168
	$ I_{BPMU203(U)} $, A	3.4469	3.4506	183.5472	166.1232	190.4675	172.8879	203.8263	175.1037
PMU203 (D)	$ V_{1PMU203(D)} $, kV	11.1005	10.1237	9.1258	7.9855	7.7301	6.076	4.7564	2.3284
	$ E_{D1} - V_{1PMU203(D)} $, kV	3.2345	4.2114	5.2147	6.3656	6.6143	8.2511	9.5962	12.0032
	$ I_{1PMU203(D)} $, A	41.9743	60.1499	67.6715	92.8073	85.8342	123.233	124.5305	183.1621
	$ I_{APMU203(D)} $, A	111.1246	152.4975	3.4451	3.5545	3.1905	3.1798	124.406	183.7132
	$ I_{BPMU203(D)} $, A	3.5672	3.5578	117.424	160.1867	121.3084	179.7569	126.0685	183.0047
	$ I_{CPMU203(D)} $, A	3.4145	3.4082	117.2816	160.4829	121.7865	179.7185	123.1511	183.1283
$Z_{U1L203} = \frac{ E_{U1} - V_{1PMU203(U)} }{ I_{1PMU203(U)} }$, Ω		$\cong 47.1347$	$\cong 47.1347$	$\cong 47.1347$	$\cong 47.1347$	$\cong 47.1347$	$\cong 47.1347$	$\cong 47.1347$	$\cong 47.1347$
$Z_{D1L203} = \frac{ E_{D1} - V_{1PMU203(D)} }{ I_{1PMU203(D)} }$, Ω		$\cong 77.059$	$\neq 77.059$	$\cong 77.059$	$\neq 77.059$	$\cong 77.059$	$\neq 77.059$	$\cong 77.059$	$\neq 77.059$
operated CBs in Line 203	phase A	yes	no	no	no	no	no	yes	no
	phase B	no	no	yes	no	yes	no	yes	no
	phase C	no	no	yes	no	yes	no	yes	no

designed MBRs along with a digital communication system. The suggested scheme can protect radial and looped micro-grids against different types of faults with the capability of single-phase tripping. In addition, since the MBRs are capable of updating their pickup values after the first change in the micro-grid configuration, they can protect micro-grid lines and buses against subsequent faults. Finally, in order to demonstrate the efficacy of the proposed protection scheme and the designed MBR, several simulations were accomplished using DigSILENT PowerFactory and MATLAB software packages.

7 References

- Georgilakis, P.S., Hatziaargyriou, N.D.: 'Optimal distributed generation placement in power distribution networks: models, methods, and future research', *IEEE Trans. Power Syst.*, 2013, **28**, (3), pp. 3420–3428
- Delghavi, M.B., Yazdani, A.: 'A control strategy for islanded operation of a distributed resource (DR) unit'. Proc. IEEE Power Energy Society General Meeting, Calgary, AB, July 2009, pp. 1–8
- Nikkhajoie, H., Lasseter, R.H.: 'Distributed generation interface to the CERTS microgrid', *IEEE Trans. Power Deliv.*, 2009, **24**, (3), pp. 1598–1608
- Baziar, A., Kavousi Fard, A.: 'Considering uncertainty in the optimal energy management of renewable micro-grids including storage devices', *Renew. Energy*, 2013, **59**, pp. 158–166
- Nthontho, M.P., Chowdhury, S.P., Winberg, S., et al.: 'Protection of domestic solar photovoltaic based microgrid'. Proc. of the 11th Int. Conf. on Developments in Power Systems Protection, Birmingham, UK, April 2012, pp. 1–7
- Li, X., Dysko, A., Burt, G.M.: 'Application of communication based distribution protection schemes in islanded systems'. Proc. of the 14th Int. Universities Power Engineering Conf. (UPEC), Cardiff, Wales, August 2010, pp. 1–6
- Zamani, M.A., Yazdani, A., Sidhu, T.S.: 'A communication-assisted protection strategy for inverter-based medium-voltage microgrids', *IEEE Trans. Smart Grid*, 2012, **3**, pp. 2088–2099
- Mirsaeidi, S., Mat Said, D., Wazir Mustafa, M., et al.: 'Progress and problems in micro-grid protection schemes', *Renew. Sust. Energy Rev.*, 2014, **37**, pp. 834–839
- Najj, W.K.A., Zeineldin, H.H., Woon, W.L.: 'Optimal protection coordination for microgrids with grid-connected and islanded capability', *IEEE Trans. Ind. Electron.*, 2013, **60**, (4), pp. 1668–1677
- Kamel, R.M., Chaouachi, A., Nagasaki, K.: 'Comparison the performances of three earthing systems for micro-grid protection during the grid connected mode', *Smart Grid Renew. Energy*, 2011, **2**, (3), pp. 206–215
- Laaksonen, H.K.: 'Protection principles for future microgrids', *IEEE Trans. Power Electron.*, 2010, **25**, (12), pp. 2910–2918
- Ustun, T.S., Ozansoy, C., Zayegh, A.: 'Modeling of a centralized microgrid protection system and distributed energy resources according to IEC 61850-70420', *IEEE Trans. Power Syst.*, 2012, **27**, (3), pp. 1560–1567
- Mirsaeidi, S., Mat Said, D., Wazir Mustafa, M., et al.: 'An analytical literature review of the available techniques for the protection of micro-grids', *Int. J. Electr. Power Energy Syst.*, 2014, **58**, pp. 300–306
- Salomonsson, D., Soder, L., Saninno, A.: 'Protection of low-voltage DC microgrids', *IEEE Trans. Power Deliv.*, 2009, **24**, (3), pp. 1045–1053
- Moeil, B., Gandomkar, M., Gooran, M., et al.: 'Distinction of permanent and transient faults in microgrids using wavelet transform', *J. Appl. Environ. Biol. Sci.*, 2013, **3**, (10), pp. 41–51
- Gopalan, S.A., Sreeram, V., Lu, H.H.C.: 'A review of coordination strategies and protection schemes for microgrids', *Renew. Sust. Energy Rev.*, 2014, **32**, pp. 222–228
- Oudalov, A., Fidigatti, A.: 'Adaptive network protection in microgrids', *Int. J. Distrib. Energy Res.*, 2009, **5**, pp. 201–225
- Dewadasa, M.: 'Protection for distributed generation interfaced networks'. BSc thesis, Electrical Engineering, Faculty of Built Environment and Engineering, Queensland University of Technology, Queensland, Australia, 2010
- Dewadasa, M., Majumder, R., Ghosh, A., et al.: 'Control and protection of a microgrid with converter interfaced micro sources'. Int. Conf. on Power Systems, 2009. ICPS '09, Kharagpur, India, December 2009, pp. 1–6
- Tumilty, R.M., Bruccoli, M., Green, T.C.: 'Approaches to network protection for inverter dominated electrical distribution systems'. The Third IET Int. Conf. on Power Electronics, Machines and Drives, 2006. PEMD 2006, Dublin, Ireland, April 2006, pp. 622–626
- Redfern, M.A., Al-Nasseri, H.: 'Protection of microgrids dominated by distributed generation using solid state converters'. Proc. of Ninth Int. Conf. on Developments in Power System Protection, Dublin, Ireland, April 2008, pp. 670–674
- Jayawarna, N., Jones, C., Barnes, M., et al.: 'Operating microgrid energy storage control during network faults'. Proc. IEEE Int. Conf. System of Systems Engineering, San Antonio, TX, April 2007, pp. 1–7
- Jayawarna, N., Jenkins, N., Barnes, M., et al.: 'Safety analysis of a microgrid'. Proc. Int. Conf. Future Power Systems, Amsterdam, Netherland, November 2005, pp. 1–7
- Sortomme, E., Venkata, S.S., Mitra, J.: 'Microgrid protection using communication-assisted digital relays', *IEEE Trans. Power Deliv.*, 2010, **25**, (4), pp. 2789–2796
- Nikkhajoie, H., Lasseter, R.: 'Microgrid protection'. Proc. IEEE Power Engineering Society General Meeting, Tampa, FL, June 2007, pp. 1–6
- Zamani, M.A., Sidhu, T.S., Yazdani, A.: 'A protection strategy and microprocessor-based relay for low-voltage microgrids', *IEEE Trans. Power Deliv.*, 2011, **26**, (3), pp. 1873–1883
- Casagrande, E., Woon, W.L., Zeineldin, H.H., Svetinovic, D.: 'A differential sequence component protection scheme for microgrids with inverter-based distributed generators', *IEEE Trans. Smart Grid*, 2013, **5**, (1), pp. 29–37
- Etetadi, A.H., Irvani, R.: 'Overcurrent and overload protection of directly voltage-controlled distributed resources in a microgrid', *IEEE Trans. Ind. Electron.*, 2013, **60**, (12), pp. 5629–5638